A Non-Cross-Bridge Stiffness in Activated Frog Muscle Fibers

Maria A. Bagni, Giovanni Cecchi, Barbara Colombini, and Francesco Colomo
Dipartimento di Scienze Fisiologiche, Università degli Studi di Firenze, I-50134 Firenze, Italy

ABSTRACT Force responses to fast ramp stretches of various amplitude and velocity, applied during tetanic contractions, were measured in single intact fibers from frog tibialis anterior muscle. Experiments were performed at 14°C at ~2.1 μm sarcomere length on fibers bathed in Ringer's solution containing various concentrations of 2,3-butanedione monoxime (BDM) to greatly reduce the isometric tension. The fast tension transient produced by the stretch was followed by a period, lasting until relaxation, during which the tension remained constant to a value that greatly exceeded the isometric tension. The excess of tension was termed "static tension," and the ratio between the force and the accompanying sarcomere length change was termed "static stiffness." The static stiffness was independent of the active tension developed by the fiber, and independent of stretch amplitude and stretching velocity in the whole range tested; it increased with sarcomere length in the range 2.1–2.8 μm, to decrease again at longer lengths. Static stiffness increased well ahead of tension during the tetanus rise, and fell ahead of tension during relaxation. These results suggest that activation increased the stiffness of some sarcomeric structure(s) outside the cross-bridges.

INTRODUCTION

It is well known that tension generation of skeletal muscle fibers during an isometric contraction is preceded by an increase of fiber stiffness starting during the latent period and continuing throughout the rise of tension (Bressler and Clinch, 1974; Cecchi et al., 1982; Ford et al., 1986). We have shown previously that most of the increase of frog muscle fiber stiffness during the latent period and the early phases of a twitch contraction is due to a sarcomere stiffness component (termed static stiffness) that did not seem to be associated with cross-bridge formation. In a single twitch the development of static stiffness followed a time course distinct from tension and resembled the internal Ca^{2+} concentration time course as measured by Ca^{2+} indicators (Bagni et al., 1994). This led us to suggest the possibility that the stiffness of some internal fiber structure(s) could increase along with intracellular Ca^{2+} concentration. We speculated that titin could be one such fiber structure. Activation could increase titin stiffness directly or it could promote a titin-actin interaction leading to a sarcomere stiffness increase. This second possibility was suggested by previous results with motility assays (Kellermayer and Granzier, 1996) showing that titin, in the presence of calcium, inhibited and even stopped the sliding of the actin filament. A calcium-modulated titin-actin interaction with mechanical effects has also been shown by Stuyvers et al. (1998) in skinned cardiac trabeculae. However, in contrast with the experiments of Kellermayer and Granzier, Stuyvers et al. found that the increase of Ca^{2+} reduced rather than increased the actin-titin interaction. These experiments give some support to the idea that titin may be involved; however, they do not exclude the possibility that static stiffness could be due to stiffening of some other structure(s), such as the actin filament. For instance, actin filament stiffness could increase as a consequence of calcium binding to troponin. The increase in actin stiffness could be transmitted to the Z lines through an interaction with other structures (titin or myosin, for example) to overcome the mechanical gap in the actin filaments at the H-band.

A limitation of our previous experiments investigating static stiffness was that they were made exclusively on twitch contractions. The lack of a steady state limited our analysis and we could not characterize most of the properties of the static stiffness. The experiments reported here, on single frog fibers during tetanic contractions, were made to overcome this limitation. The results show that the characteristics of the static stiffness are equivalent to those of a Hookean elasticity located in parallel with cross-bridges. However, this elasticity does not arise from a simple passive fiber structure because its stiffness changes upon stimulation with a characteristic time course distinct from that of tension. The maximum value of the static stiffness corresponded to <2% of the muscle fiber stiffness at tetanus plateau in normal Ringer's solution.

MATERIALS AND METHODS

Frogs (*Rana esculenta*) were killed by decapitation followed by destruction of the spinal cord. Single fibers, dissected from the tibialis anterior muscle, were mounted by means of aluminum "foil" clips (Ford et al., 1977) between the lever arms of a force transducer and an electromagnetic motor in a thermostatically controlled chamber provided with a glass floor for ordinary and laser light illumination. The temperature was maintained constant at 14°C (±0.2°C). Stimuli of alternate polarity, 0.5 ms duration and 1.5 times threshold strength, were applied transversely to the muscle fiber by means of platinum-plate electrodes. Tetanic stimulation was applied in brief (250–600 ms duration) volleys at 3-min intervals using the minimum frequency necessary to obtain fused tetani (50–60 Hz). Tension was measured by means of a capacitance force transducer (natural fre-

Submitted April 30, 2001, and accepted for publication March 5, 2002.

Address reprint requests to Dr. M. A. Bagni, Dipartimento di Scienze Fisiologiche, Università degli Studi di Firenze, Viale G. B. Morgagni, 63, I-50134 Firenze, Italy. Tel.: 39-055-4237-302; Fax: 39-055-4379-506; E-mail: mangela.bagni@unifi.it.

0006-3495/02/06/3118/10 $2.00

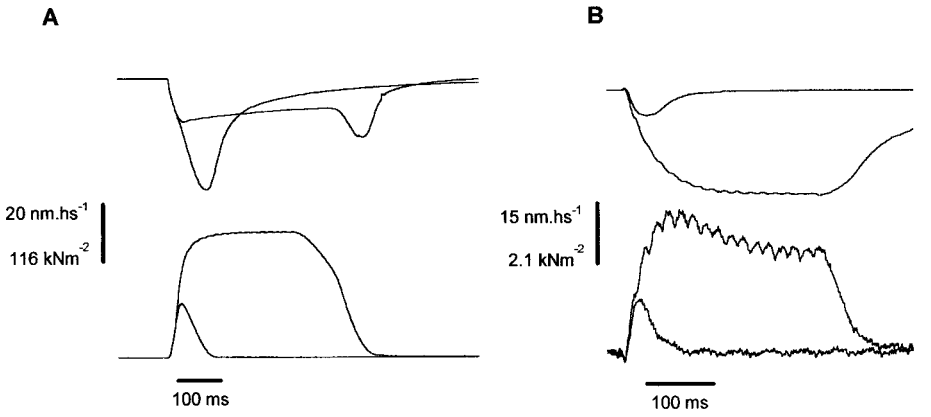

FIGURE 1 Effects of BDM on isometric twitch and tetanic contractions in a single muscle fiber at sarcomere length of 2.1 μm. Tension (*bottom traces*) and sarcomere length changes (*top traces*) in normal Ringer's solution (*A*) and in the presence of BDM (6 mM) (*B*). Note the drastic reduction of twitch and tetanic tension produced by BDM. The small drop of tension, just before the tension rise in both twitch and tetanus synchronous with the small sarcomere elongation occurring in BDM-Ringer's is the latency relaxation, which is clearly visible on this record at high amplification.

quency between 40 and 60 kHz) similar to that previously described (Huxley and Lombardi, 1980). Sarcomere length changes were measured using a striation follower device (Huxley et al., 1981) in a fiber segment (1.2–2.5 mm long) selected for striation uniformity in a region as close as possible to the force transducer. This eliminated the effects of tendon compliance on the measurements and the results could be directly attributed to the sarcomere structure. Resting sarcomere length was usually set at ~2.1 μm sarcomere length, but in a few experiments data were also collected at longer lengths (up to 3.2 μm).

After a test of fiber viability and a measure of the isometric tetanic tension (P_0) in normal Ringer's solution, all the experiments were made in Ringer's with 2,3-butanedione monoxime (BDM) added at concentration between 6 and 10 mM. The use of BDM was necessary to inhibit cross-bridge formation (Horiuti et al., 1988; Higuchi and Takemori, 1989; Lyster and Stephenson, 1995) because the relatively large and fast stretches necessary to measure the static stiffness quickly damaged fibers developing normal tetanic force (in normal Ringer's solution). In addition, cross-bridge inhibition also reduced cross-bridge contribution to the force transient evoked by the stretch, thus isolating components arising from other mechanical structures of the sarcomere. As judged by light microscopy observation and by the sarcomere length signals from the striation follower, fibers in BDM did not develop any particular sarcomere nonhomogeneity upon stretching. The fibers survived after hours of experiments with stretches and fully recovered the isometric tension when returned to normal Ringer's solution. To obtain tetanic contractions with a reasonably stable plateau in BDM-Ringer's, it was usually necessary to reduce the stimulation frequency to a point that the tetanus was slightly nonfused.

Resting fiber length, fiber cross-sectional area, and resting sarcomere length (l_0) were measured under ordinary light illumination using a 10 or 40× dry objective and 25× eyepieces. The normal Ringer's solution had the following composition (mM): 115 NaCl; 2.5 KCl; 1.8 $CaCl_2$; 3 phosphate buffer at pH 7.1. BDM-Ringer's was obtained by adding BDM at the appropriate concentration to the normal Ringer's solution. Force, fiber length, and sarcomere length signals were measured with a digital oscilloscope (Model 4094, Nicolet Instrument Corporation, Madison, WI), stored on floppy disks, and transferred to a personal computer for further analysis.

Static stiffness measurements

The method used to measure the static stiffness is the same as that described previously (Bagni et al., 1994). The activated fiber was rapidly stretched by the motor and the stretch was maintained for a period longer than the stimulation time. The tension transient produced by the stretch was followed by a period during which the tension settled to an almost constant level, which exceeded the isometric force. This level, subtracted by the tension developed at the time of the stretch and by the passive response of the fiber to the same stretch, is the static tension. The ratio between the static tension and the sarcomere length elongation produced by the stretch represents the static stiffness of the sarcomere. To follow the time course of the static stiffness development following the activation, stretches were applied in fibers at rest and at different times after the start of stimulation: during the rise of the tetanic tension, at plateau, and during the relaxation. Stretches were ramp-shaped with an amplitude up to 40 nm·hs^{-1} and 0.3–1.2 ms duration, except when we measured the effect of stretching velocity, in which case the stretch duration was increased to 30 ms. The short stretch duration, which resulted in very high stretching velocities (up to 70×10^3 nm·hs^{-1} s^{-1}), was chosen to reduce as much as possible the cross-bridge cycling during the stretch itself. The short stretch duration also reduced the time necessary for the transient to fall to the steady level at the end of the stretch (Cavagna, 1993, and Fig. 6) corresponding to the static tension.

RESULTS

For the reasons described in the Methods section, all the experiments reported here were made in fibers bathed in Ringer's solution with BDM (6–10 mM), which strongly inhibited tension generation. An example of this BDM effect is reported in Fig. 1, where twitch and tetanic tensions are reduced to only ~2% of the tensions developed in normal Ringer's solution. However, both the tension time courses and the pattern of sarcomere length changes, as measured by the striation follower, appear normal. Fig. 2 shows the effect of a stretch applied at the tetanus plateau in a fiber in BDM-Ringer's (6 mM) and illustrates the procedure followed to measure the static tension and the static stiffness. Trace *b* shows that the force increase produced by the stretch decays quickly (in ~10 ms) to a steady-state level, much greater than the isometric plateau, which remains unaltered until the end of the tetanus. The excess of the steady tension with respect to the isometric level at the time of the stretch constitutes the static tension, while the ratio between the static tension and the sarcomere elongation (trace *a*) constitutes the static stiffness. Static tension was always measured on the subtracted trace (*d*), which was obtained by subtracting the isometric force record (*c*) and the passive force response (not shown) from the force response to the stretch (*b*). The measurement was taken

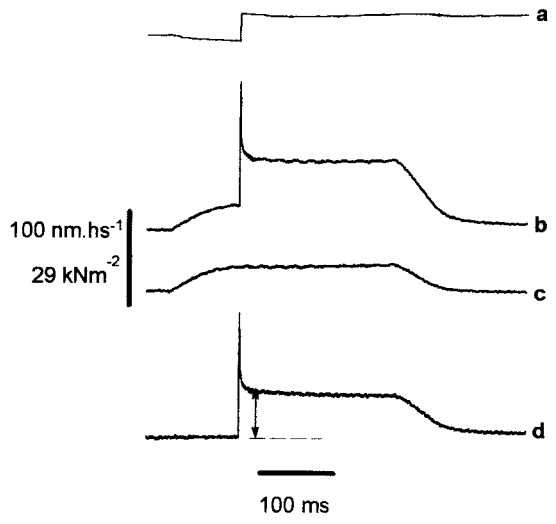

FIGURE 2 Force response to a stretch (amplitude 29.7 nm·hs^{-1}, duration 1.2 ms) applied at the tetanus plateau in a single fiber bathed in BDM-Ringer's at 6 mM concentration. (*a*) Sarcomere length; (*b*) tetanus with stretch; (*c*) isometric tetanus; (*d*) subtracted trace, obtained by subtracting the passive force response (not shown) and trace *c* from trace *b*. The static tension is measured on this trace after the end of the fast transient, as indicated by the arrow. The sarcomere length change during the isometric tetanus is not plotted.

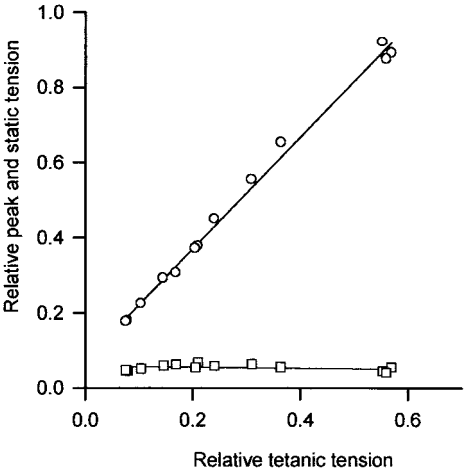

FIGURE 4 Peak tension at the break point (*circles*) and static tension (*squares*) as a function of the isometric plateau tension at the time of the stretch. Tensions are all expressed as a fraction of the tension developed at tetanus plateau in normal Ringer's solution (P_0). As expected, tension at the break point increases with the tension developed by the fiber at the time of the stretch, but static tension remains unchanged.

when the force response became steady after the transient. As can be seen in Fig. 2, the static tension is about two times greater than the isometric tension. The decay of the transient to the static force occurred roughly monoexponentially, with a time constant on the order of 5–10 ms. This response clearly differs from that obtained when a much slower stretch is applied to a fully activated fiber (Edman et al., 1982; Cavagna, 1993) where the fast recovery described above is followed by a velocity-dependent slower decaying phase. The slow phase is never present on our records with fast stretches.

In agreement with previous data (Bagni et al., 1994; Cecchi et al., 2000), the results reported here on contractions at various BDM concentrations show that static stiffness is not caused and not significantly affected by the presence of BDM. An example of this effect is reported in Fig. 3. The records in *A* show the force responses to the same stretch applied at plateau of two tetani of different amplitudes corresponding to 0.55 (*b*) and 0.08 (*c*) P_0, obtained during the slow washing of the BDM-Ringer's (8 mM) bathing solution with normal Ringer's solution. It can be seen, especially on the subtracted (and expanded) traces in *B*, that, despite the great difference in the force transients, the static tension is the same in both records. All the data from this fiber are reported in the graph of Fig. 4, showing

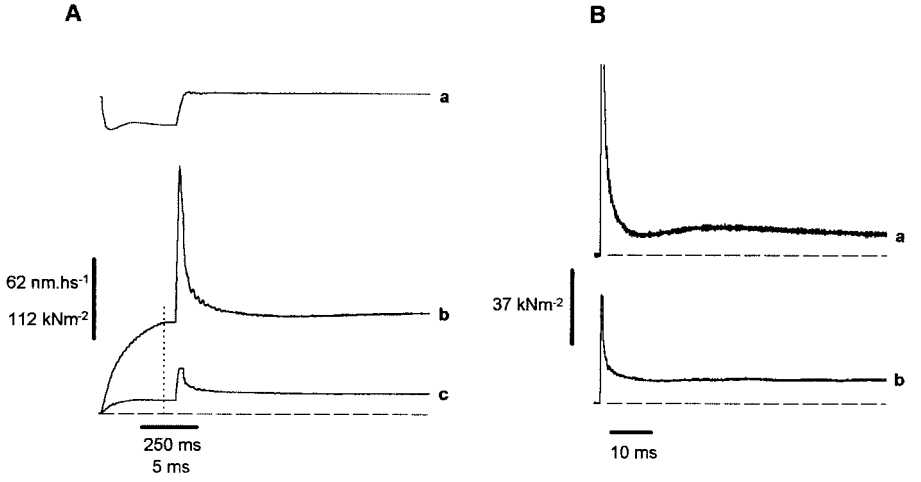

FIGURE 3 (*A*) Tension responses of a fiber to the same stretch (amplitude 32 nm·hs^{-1}, duration 0.36 ms) applied at plateau of two tetani of different amplitude. (*a*) Sarcomere length; (*b*) force response at tension of 0.55 P_0; (*c*) force response at 0.08 P_0. Tetani of different amplitude were obtained as described in the text. The vertical dashed line indicates the time of the switch from the slow to the fast time base. The horizontal dashed lines represent the resting and the plateau tension in *A* and *B*, respectively. (*B*) Subtracted traces of the same responses as in *A* (*b* and *c*) but with an expanded scale to show that the static tension is about the same in both records. Note that the slow transitory tension rise after the transient, corresponding to phase 3 of Ford et al., 1977, is present only on trace *a*.

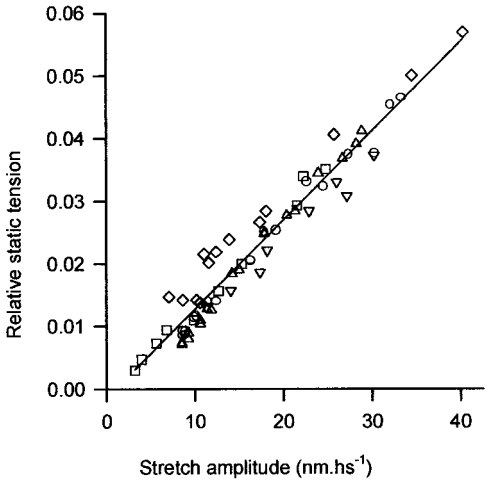

FIGURE 5 Relationships between stretch amplitude and static tension. Pooled data from five fibers. The regression line fitted on the pooled data ($r = 0.97$) is represented by the following equation: static tension = $-1.44 \times 10^{-3} + 1.42 \times 10^{-3} \times$ stretch amplitude. The angular coefficient represents the static stiffness. Different symbols refer to different fibers. Static tension is expressed relative to P_0.

the peak tension amplitude attained at the moment of the break point (Edman at al., 1978; Flitney and Hirst, 1978; Lombardi and Piazzesi, 1990; Stienen et al., 1992; Burmeister Getz et al., 1998) and the static tension as a function of the isometric plateau at which the stretch was applied. It is clear that BDM strongly affects the transient peak tension but has almost no effect on the static tension. Similar results were obtained in four different fibers.

Effects of amplitude and stretching velocity

Although our previous experiments showed that the static stiffness did not depart grossly from Hooke's law, it was not possible to show whether the static stiffness was linearly dependent on the stretch amplitude. This point was investigated here by analyzing the force response to stretches of different amplitudes, but with the same duration (0.5 ms) applied during tetanic contractions. The results from these experiments obtained on five fibers are reported as pooled data in Fig. 5. It can be seen that the relation is highly linear with an intercept close to the origin. The static tension is expressed as a fraction of P_0. The mean static stiffness, represented by the slope of the line fitted to the experimental data, was 1.42×10^{-3} P_0/nm·hs^{-1} ($\pm 0.044 \times 10^{-3}$ SE). By knowing that y_0 (the length change necessary to produce a tension change equal to P_0) at 14°C is ~5 nm·hs^{-1} (Bagni et al., 1999), it can be calculated that the stiffness of a tetanized fiber in normal Ringer's solution (S_0) is equal to 0.2 P_0/nm·hs^{-1}. This means that the static stiffness is 7.1×10^{-3} S_0 ($\pm 0.2 \times 10^{-3}$ SE), or ~1/140 of the active stiffness in normal Ringer's solution. This comparison makes clear the necessity of using stretches of great amplitude and

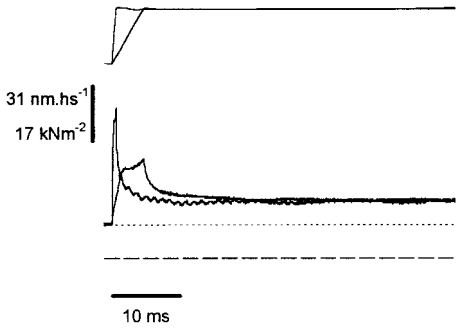

FIGURE 6 Effect of the stretching velocity on the static tension. Force responses (*bottom traces*) to stretches (*top traces*) at 31 nm·hs^{-1} amplitude at velocity of 6.6×10^3 and 48×10^3 nm·hs^{-1} s^{-1}, applied at tetanus plateau. The tension settles to the same static level in both responses, despite the differences in the force transient. The horizontal dotted and dashed lines represent the plateau and the zero tension, respectively.

reducing the cross-bridge presence to make evident the force response arising from such a small stiffness. These measurements were made at tetanus plateau, ~150 ms after the start of stimulation, when the static tension after the initial peak reached its steady-state value (see Fig. 8).

Another important point that was not analyzed in our previous report was the relation between static stiffness and stretching velocity. We report here data obtained with stretching velocities in the range 2×10^3–70×10^3 nm·hs^{-1} s^{-1} (corresponding to stretch time duration between 20 ms and 0.5 ms). Fig. 6 shows the comparison between the force response to two stretches of the same amplitude (31 nm·hs^{-1}) at speeds of 6.6×10^3 and 48×10^3 nm·hs^{-1} s^{-1} (stretch duration 4.7 ms and 0.65 ms). The two force transients are clearly different, but the static tension at which the two responses settle at the end of the transient is the same. Note the appearance of the slow decaying phase on the response to the slow stretch. Results on four fibers show that stretching velocity between the limits above do not significantly affect the static tension.

Time course of static stiffness

The time course of static stiffness development following the stimulation was determined by applying stretches with an increasing delay with respect to the start of the stimulation. An example of the force response obtained early during the tetanus rise is reported in Fig. 7. In *A* the stretch was applied 10 ms after the stimulation, when the tension developed was 0.075 the plateau tension in BDM-Ringer's (corresponding to 0.0055 P_0). It can be seen on the subtracted trace (*d*) that the static tension generated remained constant for a long period after the end of the stretch despite the noteworthy increase of the isometric tension. The same is true in Fig. 7 *B*, in which the stretch was applied 6 ms after the stimulation when the active isometric tension (*c*) was very nearly zero. Note that in *A* at the end of the stretch,

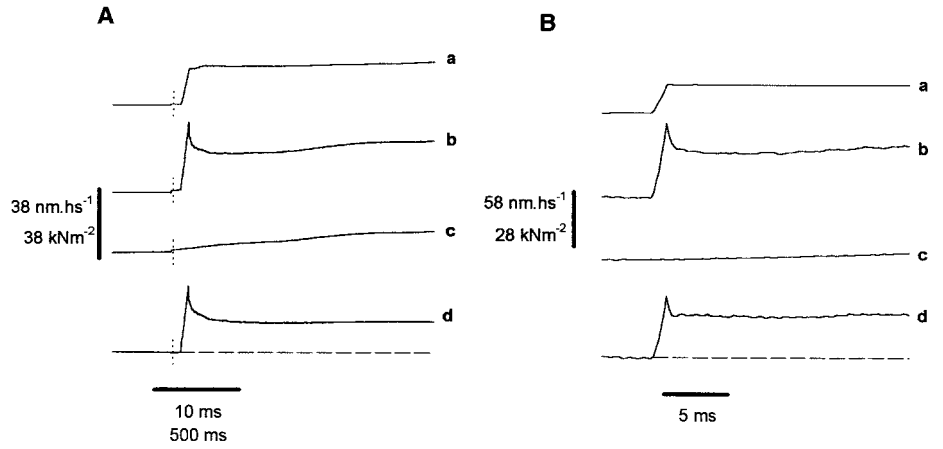

FIGURE 7 Tension responses to stretches applied on the tetanus rise (*A*) and during the latent period (*B*). (*a*) Sarcomere length; (*b*) tetanus with stretch; (*c*) isometric tetanus; (*d*) subtracted trace. (*A*) Stretch applied 10 ms after the start of stimulation at a tension of 0.006 P_0. Note on trace *d* that the tension following the stretch settles to a level that remains constant for the rest of the record, despite the significant increase that occurs during the same time in the isometric tension. (*B*) Stretch applied 6 ms after the stimulation, when the tension developed was very nearly zero. The subtracted trace *d* shows that by this time the static tension has already reached a considerable value (80% of the maximum). Note that after a sharp peak at the end of the stretch the tension settles quickly to the static value. The peak is instead followed by a slower phase in (*A*), which is likely due to the reversal of the power stroke of the stretched cross-bridge. The vertical lines in *A* mark the change from the slow to the fast time base.

similar to other responses shown previously, the force settles almost exponentially to the static level in a few milliseconds, very likely through the mechanism of the quick force recovery of the few cross-bridges attached. However, in *B* the active tension is zero at the time of the stretch, and no force generating cross-bridges are present. Consequently, the quick recovery is absent from the force transient, and the response of the static stiffness stands alone (the small peak at the end of the stretch, which decays completely in <400 μs, is very likely an inertial effect due to the fast stretch and the low stiffness of the fiber in the absence of cross-bridges). The records in Fig. 7 *B* illustrate three important points about the static tension: 1) it is already present during the latent period when the active tension is zero; 2) it is established with no delay immediately after the end of the stretch; and 3) it remains constant afterward even if the isometric tension is changing. Thus the static tension and the corresponding static stiffness can be attributed to the time of the stretch application, independent of the time at which the static tension was effectively measured. The complete time courses of static stiffness and tension during a twitch and a tetanic contraction are reported in Fig. 8 *A*. The static stiffness development (*top traces*) clearly precedes the active tension (*bottom traces*), as it begins to rise 3 ms after the stimulus at the beginning of the latency relaxation. During the relaxation, static stiffness also leads active tension, as it starts to decline well ahead of tension. The peak stiffness value in both twitch and tetanus was reached at ~8–12 ms after the start of stimulation, when the tension had just started to rise (Fig. 8 *B*). After the peak the stiffness decreased to zero in ~50 ms in the twitch, while in the tetanus it decayed within 100–200 ms to a plateau level maintained until the start of relaxation. In six fibers the mean stiffness at plateau was 1.24×10^{-3} P_0/nm·hs^{-1} ($\pm 0.12 \times 10^{-3}$ SE) (at a mean tension of 0.0363 P_0 (± 0.0038 SE)), while the mean peak stiffness was 3.24×10^{-3} P_0/nm·hs^{-1}($\pm 0.6 \times 10^{-3}$ SE) (at a mean tension of 0.0042 P_0 (± 0.0015 SE)). The value at steady state for these six fibers is not statistically different from the value reported in Fig. 5 obtained from a different group of six fibers. The mean static stiffness was therefore ~2.5 times greater at the peak than at the steady state, corresponding to ~1.6% of the total fiber stiffness in normal Ringer's solution.

To illustrate the effect of the activation on static stiffness it is interesting to compare the force responses to the same stretch applied at the same tension level on the tetanus rise and during relaxation. An example of this comparison, reported in Fig. 9, shows that the static tension is quite different in the two cases, being 0.044 P_0 on the rise and 0.0014 P_0 on the relaxation. This is a clear demonstration that static tension is not correlated with active tension, but depends on other aspects of fiber activation.

Effects of sarcomere length

In a few experiments, the time course of static stiffness development was measured at different sarcomere lengths in a range between 2.1 and 3.2 μm. Fig. 10 reports an example of results at 2.2 μm and 2.8 μm sarcomere length. It can be seen that static stiffness increased substantially when sarcomere length was increased, while its time course changed only slightly. The 3.5-fold static stiffness increase

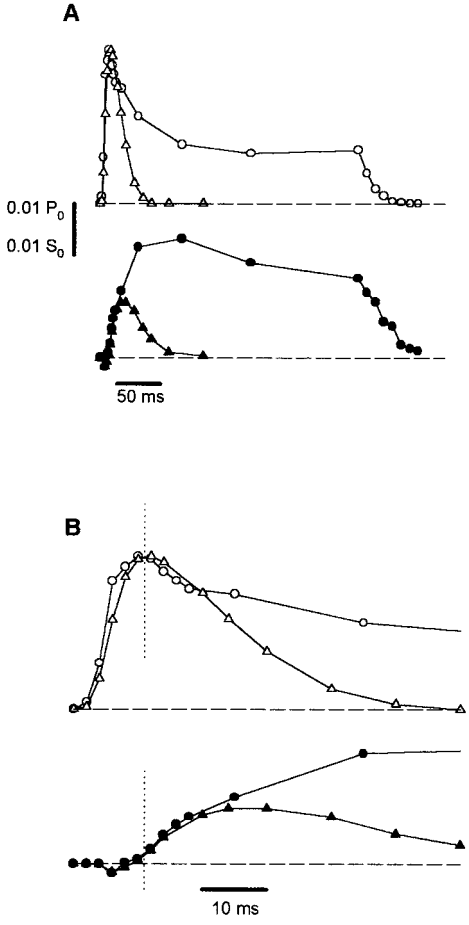

FIGURE 8 Time course of static stiffness development following the stimulation in twitch and tetanic contractions. (*A*) Whole time course of tension (*bottom traces*, *filled symbols*) and static stiffness (*top traces*, *empty symbols*) in twitch (*triangles*) and tetanic contractions (*circles*). The data refer to the active tension developed at the time of the stretch and to the corresponding static stiffness measured in different contractions in which stretches were applied at different times after the start of stimulation. Both tension and static stiffness values are expressed relative to the plateau values in normal Ringer's solution. Stiffness rises ahead of tension during the tetanus rise and falls ahead of tension during relaxation. (*B*) Initial part of *A* at a faster time base. The dashed lines indicate the resting tension. The small drop of force below the resting value, preceding the force generation, represents the latency relaxation. Note that the peak of static stiffness (indicated by the vertical dotted line) is reached ~10 ms after the start of stimulation (coincident with the first point plotted) when tension is still very small. Sarcomere length: 2.1 μm.

occurred despite a substantial decrease (45%) in myofilament overlap. Static stiffness reached the maximum value at sarcomere lengths around 2.6–2.8 μm to decrease again at longer length (data not reported). It is interesting to note that the sarcomere length dependence of the static stiffness is about the same as that of the latency relaxation (Bagni et al., 1996). Together with the observation that static stiffness starts to rise at the same time as the latency relaxation, this finding suggests a possible correlation between the two phenomena.

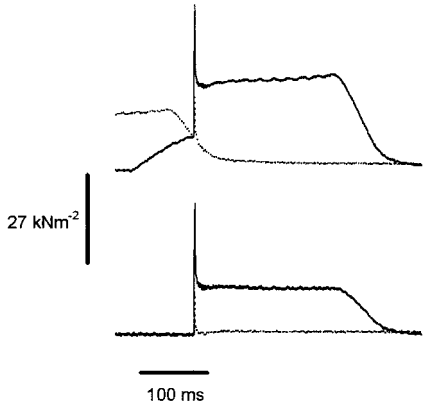

FIGURE 9 Force responses to a stretch (amplitude 33.7 $nm \cdot hs^{-1}$, duration 0.6 ms) applied at the same tension level (~50% of the maximum) during the tetanus rise (*thick lines*) and the relaxation (*dotted thin lines*) in two tetanic contractions on the same fiber. Top records, tetani with stretches; bottom records, subtracted traces. Note that the static tension is clearly present on the tetanus rise, but is almost absent on the relaxation.

DISCUSSION

In agreement with previous data on twitch contractions (Bagni et al., 1994), the experiments reported in this paper show that the tension transient produced by fast stretches applied to tetanized single muscle fibers bathed in BDM-Ringer's is followed by a period during which the tension stays constant to a level well above the isometric tension. This excess of tension, referred to as static tension, persists until the relaxation and is attributable to the elongation of some elastic element of the sarcomere whose stiffness changes characteristically following fiber activation. BDM was used throughout all the present experiments to inhibit tension generation and greatly reduce the effect of cross-bridge stretching on the force response. This protocol was adopted on the assumption that static tension is not caused by and not affected by the presence of BDM. The validity of this assumption is demonstrated by our previous data show-

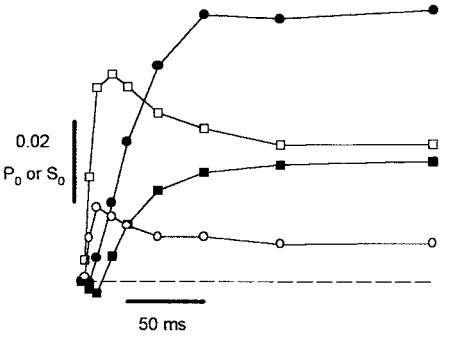

FIGURE 10 Time courses of isometric tension (*filled symbols*) and static stiffness (*empty symbols*) at 2.2 μm (*circles*) and 2.8 μm (*squares*) sarcomere length. Note that static stiffness increases ~3.5 times at 2.8 μm despite a 45% reduction of filament overlap.

ing that 1) static tension is present in normal Ringer's solution and with the same value as that found in BDM-Ringer's (Bagni et al., 1994); and 2) static tension is present in tetanic contractions in which methanol is used to inhibit tension generation (Cecchi et al., 2000). Additional evidence is provided by the results reported here showing the independence of the static stiffness from BDM concentration up to 10 mM. BDM has been shown to have several effects on muscle contraction, the most important of which are a direct inhibition of actomyosin interaction and a reduction of calcium released upon stimulation (Fryer et al., 1988; Horiuti et al., 1988; Higuchi and Takemori, 1989; Lyster and Stephenson, 1995; Maylie and Hui, 1991; Tripathy et al., 1999). However, these effects are strongly species-dependent. In frog intact fibers (our preparation) the main effect of BDM at concentrations up to 10 mM is a dose-dependent inhibition of actomyosin interaction, while the effect on calcium release has been shown to be minimal (Horiuti et al., 1988; Maylie and Hui, 1991; Sun et al., 2001).

Characteristics of static stiffness

Figs. 5 and 6 show that static tension depends linearly on the stretch amplitude and is independent of the stretching speed. In these experiments the stretch amplitude varied in a range between 2 and 40 nm·hs^{-1}, which included the sarcomere elongation (10–14 nm·hs^{-1}) necessary to reach the break point on the force response. The attainment of this length did not correspond to any change on the slope of the stretch amplitude-static tension relation, which maintained its linearity in the whole range tested. These properties indicate that within the limits of our experiments the elasticity of the structure responsible for the static stiffness is Hookean and undamped. The observation that after the end of the stretch the static tension remains constant for the entire stimulation time indicates that the static stiffness is not associated with a significant relaxation time. Based on these combined observations we can assume that static stiffness arises from a pure elastic structure.

Static stiffness time course

Data from Fig. 8 show that the development of static stiffness following stimulation is clearly distinct from tension development. The static stiffness begins to rise ~2–3 ms after the start of stimulation when the active tension is still zero, and peaks at ~10 ms after the stimulus when the tension is still very small. After the peak, the static stiffness decreases in ~100–200 ms to a plateau maintained until the start of relaxation. During this period the fiber develops the maximum force. It is clear that, similar to what was observed with the measurements at plateau of tetani of different amplitudes, static stiffness and active tension are uncorrelated. A similar dissociation is observed during tetanus relaxation (Figs. 8 and 9) where the fall of static stiffness precedes tension fall.

Mechanisms responsible for the static stiffness

The most striking feature of the static stiffness resulting from our analysis is its complete independence from the active tension developed by the fiber. This occurred in all the conditions in which tension was altered, for example, by adding different amounts of BDM, or by changing the filament overlap, or during the tetanus rise or relaxation. Particularly important is the finding that static stiffness is well established even during the latent period, when the force developed by the fiber is zero. These observations indicate that static tension does not arise from stretching of force-generating cross-bridges. Consistent with this view is the finding that the static tension, once generated at the end of the stretch, remained constant for the entire stimulation time (at least 250 ms in our experiments). This time is far greater than the time (a few milliseconds) needed for the stretched cross-bridges to restore their unstrained configuration by reversing the force-generating step (Ford et al., 1977) and much greater than the time of repriming of the initial conditions after a stretch (Piazzesi et al., 1997). Therefore, the stretched cross-bridges cannot contribute to the excess of tension above the isometric. Recent experiments by Burmeister Getz et al. (1998) suggest that the force response to slow stretching of rabbit skinned fibers arises mainly from weakly bound bridges. This raises the question of whether our response could be due to stretching of weakly binding bridges, especially since BDM has been shown to convert strongly bound bridges into weakly bound bridges (Herrmann et al., 1992). However, due to their fast attachment-detachment kinetics (Schoenberg, 1985), weakly binding bridges should contribute to the force response only dynamically during the stretch itself, their force response being similar to that of a viscoelastic element (compliance in series with a dashpot). At the end of the length change, the stretched weakly bound bridges rapidly detach with a rate constant of $\sim 10^4$ s^{-1} (Schoenberg, 1985) and consequently, their force reduces to zero in less than a millisecond. Thus, while weakly binding bridges can generate a substantial portion of the force response during the stretch, they cannot sustain a steady increase of tension such as that constituted by the static tension. On the assumption that BDM increases the number of weak binding bridges, the observation that static stiffness is the same in normal and BDM-Ringer's (Bagni et al., 1994) confirms that this parameter is not due to weakly binding bridges.

In general, even if we assume slow cross-bridge kinetics, it seems unlikely that stretching of attached cross-bridges could be responsible for the static stiffness. For example, to explain the linearity of the relation between static tension and stretch amplitude and the absence of a breaking point,

we should assume that these cross-bridges can be stretched up to 40 nm·hs^{-1} without detaching.

A possible explanation for the static stiffness involving cross-bridges is that the stretch could promote the formation of freshly attached bridges, which will then add their force to the isometric tension at the end of the stretch. This possibility cannot be excluded; however, the following observations make it unlikely. The records in Fig. 7 *B* show that the static tension produced by stretching a fiber during the latent period reaches the steady value just at the end of the stretch, with no appreciable delay. This means that cross-bridge formation possibly promoted by the stretch should occur with a very high rate constant, $>2 \times 10^3$ s^{-1}. In addition, because in this record there is no quick force recovery at the end of the stretch, we should also assume that these freshly formed cross-bridges are unstrained at the end of the stretch. Both assumptions seem unlikely. Further evidence pointing to the same conclusion is reported in Fig. 3, in which we compared the responses to stretches applied at two different isometric levels, 0.55 and 0.08 P_0. The slow tension rise following the quick drop at the end of the stretch (phase 3 of Ford et al., 1977), which has been attributed to freshly attached cross-bridges, is present on the force response evoked at high isometric tension, but it is absent on the transient at low isometric tension. Nevertheless, both records have about the same static tension. This suggests that if cross-bridge attachment occurs during the stretch under our conditions, it probably makes a small contribution to the static tension.

Despite the very different conditions under which the experimental responses are obtained, it may be interesting to compare the properties of the static tension reported here with those of post stretch potentiation previously described (Sugi, 1972; Cavagna and Citterio, 1974; Edman et al., 1978; Julian and Morgan, 1979; Sugi and Tsuchiya, 1981; Morgan, 1990; Noble, 1992, and further references therein) which occurs when slow stretches (about two orders of magnitude slower that those used here) are applied at plateau of fully activated fibers under Ringer's solution. The post stretch potentiation is constituted by two main components: 1) a velocity-dependent increase of force that decays after the stretch within a few seconds; and 2) a second component, referred to as "residual force enhancement post-stretch," increasing linearly with the stretch amplitude and independent of stretching velocity, which persists to the end of a long tetanus (Edman et al., 1982; Edman and Tsuchiya, 1996). Our records show that force decays at the end of the stretch, almost exponentially in ~10 ms to the steady level with no sign of the slowly decaying first component. The absence of this phase, which has been attributed to the increased strain of attached cross-bridges and possibly to a slight increase in cross-bridge number (Edman et al., 1978, 1982; Sugi and Tsuchiya, 1981; Lombardi and Piazzesi, 1990; Linari et al., 2000), gives further support to the idea that static stiffness does not arise from cross-bridges.

The observation that static tension is independent of velocity, increases linearly with stretch amplitude, and does not decay until the end of the stimulation, suggests a possible analogy with the residual force enhancement. Static tension and residual force enhancement are also similar with regard to their dependence on sarcomere length and their occurrence with no delay after the end of the stretch. The only important difference suggesting that the two phenomena are not necessarily equal is that the residual enhancement after stretch is present only on the descending limb of the length-tension relation, and not at plateau (Edman et al., 1982). This is not the case with the static tension, which is clearly evident at the 2.1 μm sarcomere length at which we made our experiments. The many similarities between static tension and residual force enhancement raises the possibility that static tension results from sarcomere length nonuniformity along the fiber and/or within the fiber volume, as hypothesized for the mechanism of residual force enhancement (Edman and Tsuchiya, 1996). Edman and Tsuchiya suggested that small differences in force developed by adjacent myofibrils could lead to a strain of some elastic elements of the fiber, which will be further strained by the stretch leading to a force potentiation. It is clear that this kind of potentiation will occur only when the stretch is applied to a fiber-generating active force. For this reason it is unlikely that this mechanism could be responsible for the static tension, which is well developed in complete absence of force during the latent period. In addition, we show here that static stiffness drops substantially during relaxation, when it is known that a noteworthy sarcomere length nonuniformity is occurring.

Our static stiffness data can be explained by assuming the presence of a structure in parallel with the cross-bridges behaving like a linear "spring." This would not be a simple passive elastic component because its stiffness is variable with time after the stimulation and it does not depend on tension. The force response to the stretch of an activated fiber would therefore be composed of at least two components, one due to the cross-bridges and the other due to the unknown elastic structure(s) responsible for the static stiffness. Titin could constitute one of such structure. Upon stimulation, titin stiffness could increase directly or it could interact with actin, leading to an increase of sarcomere stiffness. Some observations reported recently seem to lend support to this second possibility. Data from motility assays (Kellermayer and Granzier, 1996) have shown that the sliding movement of actin filaments can be inhibited and even stopped by the presence of titin in the medium, an effect that was attributed to a titin-actin interaction. It is interesting that this interaction occurred in a calcium-dependent manner: increased calcium in fact resulted in a greater suppression of in vitro motility. A calcium dependent titin-actin interaction leading to a sarcomere stiffness increase was also found by Stuyvers et al. (1998) in cardiac trabeculae. In fact, the stiffness changes found by these authors

during the diastolic phase could be abolished by adding to the bathing solution a cloned fragment of titin (Ti-II), which strongly interacts with f-actin (Jin, 1995). However, in this case, calcium inhibits rather than activates titin-actin interaction. Because titin is firmly anchored to Z lines and myosin filaments, a mechanical connection with actin in the I-band region could increase the stiffness of portions of the titin filament, thus accounting for the static stiffness increase. It might also be possible that the formation of these links is responsible for the small force drop and the small sarcomere lengthening (Haugen and Sten-Kundsen, 1976; Bagni et al., 1996) that occur during the latency relaxation. The increase of static stiffness at longer sarcomere lengths (up to 2.6–2.8 μm) and the subsequent decrease at longer lengths could be attributed to a modulating effect of other factors such as lateral myofilament separation, titin stretching, and overlap between titin and free actin.

Given the low value of the static stiffness, which at most is $<2\%$ of the total activated fiber stiffness, a titin-actin interaction (or a titin stiffness increase) would not significantly impair cross-bridge performance during normal contractions. However, static stiffness could play an important role in maintaining the stability of the sarcomere structure at the beginning of activation when few cross-bridges are attached, perhaps nonuniformly, along the sarcomere as a consequence of the nonuniform intracellular Ca^{2+} distribution (Escobar et al., 1994). It is interesting that this stabilizing action would occur with appropriate timing, just before and at the very early phases of force development.

All the above considerations do not exclude and could be applied to other possible candidates for the increase in sarcomere stiffness upon activation. Actin filament stiffness, for instance, could increase upon calcium binding to troponin or troponin movement. The continuity gap in the actin filament at the H-band, which would not allow the actin stiffness to be transmitted at Z lines, could be overcome by mechanical connections between actin and some other structure(s), possibly myosin or titin.

REFERENCES

Bagni, M. A., G. Cecchi, E. Cecchini, F. Colomo, and P. Garzella. 1996. Sarcomere length dependence of frog muscle fibre stiffness during the latent period. *Pflügers Arch.* 431.6:R333.

Bagni, M. A., G. Cecchi, B. Colombini, and F. Colomo. 1999. Sarcomere tension-stiffness relation during the tetanus rise in single frog muscle fibres. *J. Muscle Res. Cell Motil.* 20:469–476.

Bagni, M. A., G. Cecchi, F. Colomo, and P. Garzella. 1994. Development of stiffness precedes cross-bridge attachment during the early tension rise in single frog muscle fibers. *J. Physiol.* 481.2:273–278.

Bressler, B. H., and N. F. Clinch. 1974. The compliance of contracting skeletal muscle. *J. Physiol.* 237:477–493.

Burmeister Getz, E., R. Cooke, and S. L. Lehman. 1998. Phase transition in force during ramp stretches of skeletal muscle. *Biophys. J.* 75: 2971–2983.

Cavagna, G. A. 1993. Effect of temperature and velocity of stretching on stress relaxation of contracting frog muscle fibres. *J. Physiol.* 462: 161–173.

Cavagna, G. A., and G. Citterio. 1974. Effect of stretching on the elastic characteristics and the contractile component of frog striated muscle. *J. Physiol.* 239:1–14.

Cecchi, G., M. A. Bagni, B. Colombini, and R. Garuglieri. 2000. Force response to fast ramp stretches of activated frog muscle fibres in presence of methanol. *Biophys. J.* 78:119*a*. (Abstr.).

Cecchi, G., P. J. Griffiths, and S. Taylor. 1982. Muscular contraction: kinetics of crossbridge attachment studied by high-frequency stiffness measurements. *Science.* 217:70–72.

Edman, K. A. P., G. Elzinga, and M. I. M. Noble. 1978. Enhancement of mechanical performance by stretch during titanic contractions of vertebrate skeletal muscle fibres. *J. Physiol.* 281:139–155.

Edman, K. A. P., G. Elzinga, and M. I. M. Noble. 1982. Residual force enhancement after stretch of contracting frog single muscle fibers. *J. Gen. Physiol.* 80:769–784.

Edman, K. A. P., and T. Tsuchiya. 1996. Strain of passive elements during force enhancement by stretch in frog muscle fibres. *J. Physiol.* 490.1: 191–205.

Escobar, A. L., J. R. Monck, J. M. Fernandez, and J. L. Vergara. 1994. Localization of the site of Ca^{2+} release at level of a single sarcomere in skeletal muscle fibre. *Nature.* 367:739–741.

Flitney, F. W., and D. G. Hirst. 1978. Crossbridge detachment and sarcomere "give" during stretch of active frog's muscle. *J. Physiol.* 276: 449–465.

Ford, L. E., A. F. Huxley, and R. M. Simmons. 1977. Tension responses to sudden length changes in stimulated frog muscle fibres near slack length. *J. Physiol.* 269:441–515.

Ford, L. E., A. F. Huxley, and R. M. Simmons. 1986. Tension transients during the rise of tetanic tension frog muscle fibres. *J. Physiol.* 372: 595–609.

Fryer, M. W., I. R. Neering, and D. G. Stephenson. 1988. Effects of 2,3-butanedione monoxime on the contractile activation properties of fast- and slow-twitch rat muscle fibres. *J. Physiol.* 407:53–75.

Haugen, P., and O. Sten-Kundsen. 1976. Sarcomere lengthening and tension drop in the latent period of isolated frog skeletal muscle fibres. *J. Gen. Physiol.* 68:247–265.

Herrmann, C., J. Wray, F. Travers, and T. Barman. 1992. The effect of 2,3-butanedione monoxime on myosin and myofibrillar ATPases. An example of an uncompetitive inhibitor. *Biochemistry.* 31:12227–12232.

Higuchi, H., and S. Takemori. 1989. Butanedione monoxime suppresses contraction and ATPase activity of rabbit skeletal muscle. *J. Biochem.* 105:638–643.

Horiuti, K., H. Higuchi, Y. Umazume, M. Konishi, O. Okazaki, and S. Kurihara. 1988. Mechanism of action of 2,3-butanedione 2-monoxime on contraction of frog skeletal muscle. *J. Muscle Res. Cell Motil.* 9:156–164.

Huxley, A. F., and V. Lombardi. 1980. A sensitive force transducer with resonance frequency 50 kHz. *J. Physiol.* 305:15–16.

Huxley, A. F., V. Lombardi, and L. D. Peachey. 1981. A system for fast recording of longitudinal displacement of a striated muscle fibre. *J. Physiol.* 317:12–13.

Jin, J. P. 1995. Cloned rat cardiac titin class I and class II motifs. Expression, purification, characterization, and interaction with F-actin. *J. Biol. Chem.* 270:1–9.

Julian, F. J., and D. L. Morgan. 1979. The effect on tension of nonuniform distribution of length changes applied to frog muscle fibres. *J. Physiol.* 293:379–392.

Kellermayer, M. S. Z., and H. L. Granzier. 1996. Calcium-dependent inhibition of in vitro thin-filament motility by native titin. *FEBS Lett.* 380:281–286.

Linari, M., L. Lucii, M. Reconditi, M. E. Vannicelli Casoni, H. Amenitsch, S. Bernstorff, G. Piazzesi, and V. Lombardi. 2000. A combined mechanical and x-ray diffraction study of stretch potentiation in single frog muscle fibres. *J. Physiol.* 526.3: 589–596.

Lombardi, V., and G. Piazzesi. 1990. The contractile response during steady lengthening of stimulated frog muscle fibres. *J. Physiol.* 431: 141–171.

Lyster, D. J., and D. G. Stephenson. 1995. Contractile activation and measurements of intracellular Ca^{2+} concentration in cane toad twitch fibres in the presence of 2,3-butanedione monoxime. *Exp. Physiol.* 80:543–560.

Maylie, J., and C. S. Hui. 1991. Action of 2,3-butanedione monoxime on calcium signals in frog cut twitch fibres containing antipyrylazo III. *J. Physiol.* 442:551–557.

Morgan, D. L. 1990. New insights into the behaviour of muscle during active lengthening. *Biophys. J.* 57:209–221.

Noble, M. I. M. 1992. Enhancement of mechanical performance of striated muscle by stretch during contraction. *Exp. Physiol.* 77:539–552.

Piazzesi, G., M. Linari, M. Reconditi, F. Vanzi, and V. Lombardi. 1997. Cross-bridge detachment and attachment following a step stretch imposed on active single frog muscle fibres. *J. Physiol.* 498:3–15.

Schoenberg, M. 1985. Equilibrium muscle cross-bridge behavior: theoretical considerations. *Biophys. J.* 48:467–475.

Stienen, G. J. M., P. G. A. Versteeg, Z. Papp, and G. Elzinga. 1992. Mechanical properties of skinned rabbit psoas and soleus muscle fibres during lengthening: effects of phosphate and Ca^{2+}. *J. Physiol.* 451: 503–523.

Sugi, H. 1972. Tension changes during and after stretch in frog muscle fibres. *J. Physiol.* 225:237–253.

Sugi, H., and T. Tsuchiya. 1981. Enhancement of mechanical performance in frog skeletal muscle fibres after quick increases in load. *J. Physiol.* 319:239–252.

Stuyvers, B. D., M. Miura, J. P. Jin, and H. E. D. J. ter Keurs. 1998. Ca^{2+}-dependence of diastolic properties of cardiac sarcomeres: involvement of titin. *Prog. Biophys. Mol. Biol.* 69:425–443.

Sun, Y. B., F. Lou, and K. A. P. Edman. 2001. 2,3-Butanedione monoxime increases speed of relaxation in single muscle fibers of frog. *Acta Physiol. Scan.* 172:53–61.

Tripathy, A., L. Xu, D. A. Pasek, and G. Meissner. 1999. Effects of 2,3-butanedione 2-monoxime on Ca^{2+} release channels (ryanodine receptors) of cardiac and skeletal muscle. *J. Membr. Biol.* 169:189–198.